

Article

Transient Axisymmetric Flows of Casson Fluids with Generalized Cattaneo's Law over a Vertical Cylinder

Husna Izzati Osman ¹, Dumitru Vieru ²  and Zulhibri Ismail ^{1,*} 

¹ Centre for Mathematical Sciences, Universiti Malaysia Pahang, Lebuhraya Tun Razak, Gambang 26300, Pahang, Malaysia; husnaizzatii@yahoo.com

² Department of Theoretical Mechanics, Technical University of Iasi, 700050 Iasi, Romania; dumitru_vieru@yahoo.com or dumitru.vieru@tuiasi.ro

* Correspondence: zulhibri@ump.edu.my

Abstract: Unsteady axial symmetric flows of an incompressible and electrically conducting Casson fluid over a vertical cylinder with time-variable temperature under the influence of an external transversely magnetic field are studied. The thermal transport is described by a generalized mathematical model based on the time-fractional differential equation of Cattaneo's law with the Caputo derivative. In this way, our model is able to highlight the effect of the temperature gradient history on heat transport and fluid motion. The generalized mathematical model of thermal transport can be particularized to obtain the classical Cattaneo's law and the classical Fourier's law. The comparison of the three models could offer the optimal model of heat transport. The problem solution has been determined in the general case when cylinder surface temperature is described by a function $f(t)$; therefore, the obtained solutions can be used to study different convective flows over a cylinder. In the particular case of surface temperature varying exponentially in time, it is found that fractional models lead to a small temperature rise according to the Cattaneo model.

Keywords: Casson fluids; Cattaneo's law; Caputo fractional derivative



Citation: Osman, H.I.; Vieru, D.; Ismail, Z. Transient Axisymmetric Flows of Casson Fluids with Generalized Cattaneo's Law over a Vertical Cylinder. *Symmetry* **2022**, *14*, 1319. <https://doi.org/10.3390/sym14071319>

Academic Editor: Mikhail Sheremet

Received: 27 May 2022

Accepted: 23 June 2022

Published: 26 June 2022

Publisher's Note: MDPI stays neutral with regard to jurisdictional claims in published maps and institutional affiliations.



Copyright: © 2022 by the authors. Licensee MDPI, Basel, Switzerland. This article is an open access article distributed under the terms and conditions of the Creative Commons Attribution (CC BY) license (<https://creativecommons.org/licenses/by/4.0/>).

1. Introduction

Casson liquids are suitable for heating/cooling operations due to its efficient impact on the energy transmission rate. The rheological model of Casson fluid [1], used to model the flow of pigment suspensions in the production of printing ink, is also capable of effectively describing the flow characteristics of polymers, human blood, starch suspensions, foams, molten cosmetics, paints, synthetic lubricants etc. [2]. In view of the multiple practical applications of the Casson fluids, several studies have been conducted on flows of these fluids.

Unsteady flows of a viscous, incompressible and electrically conducting Casson fluid past a moving vertical cylinder with time-variable temperature under the impact of mass diffusion, transversely uniform magnetic field, and chemical reaction have been studied by Kumar and Rizvi [3]. Using a numerical scheme based on the Crank-Nicolson implicit finite differences, the authors analyzed fluid motion and heat and mass transfer.

Reddy et al. [4] numerically studied the entropy generation in the heat and momentum transfer in time-dependent boundary layer flow of a Casson viscoplastic fluid over a uniformly heated vertical cylinder embedded in an isotropic, homogenous porous medium. The hydrodynamic flow of incompressible Casson fluids over a yawed cylinder is investigated by Khan et al. [5] using the homotopy analysis method. Sarkar et al. [6] investigated magnetohydrodynamics boundary layer flows of Casson and Williamson nanofluids over an inclined cylindrical surface. The impact of linear order chemical reaction and thermal radiation has been considered in the mathematical model.

The flow of Casson fluids mixed with nano size metallic particles, under the influence of an external magnetic field and thermal radiation, owing to a moving boundary cylinder

have been studied by Naqvi et al. [7]. The Joule heating and dissipation are considered in convective heat transfer. Numerical solutions of the governing equations have been obtained and results are presented in graphical illustrations to analyze the fluid motion and heat transfer. Ullah et al. [8] have studied flows of Casson fluids over a non-isothermal cylinder subject to suction/blowing and to the nonlinear stretching. The effects of porous medium, chemical reaction, viscous dissipation, and heat generation/absorption on the flow fields have been considered in this study. The numerical solutions are obtained using the similarity transformations and the Keller box method.

The classical heat flow, based on the Fourier law leads to a parabolic differential equation of heat transfer. Later, some nonclassical theories of heat flow described by hyperbolic-type equations have been developed.

Recent developments in technology of measurements highlighted some anomalous in heat transport that cannot be explained by the classical mathematical models of heat transport. Researchers in the field of heat transfer have developed other mathematical models that are able to describe the complex phenomena of diffusion processes. So, the mathematical models of heat transfer based on constitutive equations with fractional derivatives in time or space have been developed and studied.

The models using fractional derivatives are considered to be an excellent tool for describing the memory and hereditary properties of various materials and processes [9]. For these reasons, the fractional models are used in the modeling of various phenomena in thermoelasticity, physics, mechanics, control theory, biochemistry, bioengineering, economics, etc. Povstenko [10] proposed a quasi-static uncoupled theory of thermoelasticity based on the heat conduction equation with a time-fractional Caputo derivative. The thermal stresses corresponding to the fundamental solutions of a Cauchy problem for the fractional heat conduction equation are found in one-dimensional and two-dimensional cases. An interesting review about anomalous energy transport in one dimensional region and several models of the non-local fractional heat conduction can be found in the reference [11]. The maximum temperature propagation in a finite medium using a single-phase-lag of heat equation with fractional Caputo derivatives has been studied by Kukla and Siedlecka [12]. The authors proposed Robotnov functions and a harmonically ambient temperature to study the heat source problems. The problem has been solved by using the eigenfunction expansion method and the Laplace transform technique with time-dependent Robin and homogenous Neumann boundary conditions. The obtained solutions were used for determination of the maximum temperature trajectories. Liu et al. [13] have investigated the influence of the hall effect and radiation heat on unsteady fractional Maxwell fluids of magnetohydrodynamic flows and heat transfer in a square cavity. The coupled model is formed from the momentum equation based on the Fourier law derivation of fractional heat-conduction equation and the fractional constitutive relationship. They obtained numerical solutions using the weighted and shifted Grünwald difference method in the temporal direction with the spectral method based on Lagrange-basis polynomials in the spatial direction. The stability and convergence of the numerical schemes are proved. Wang et al. [14] formulated a finite difference algorithm on bioheat transfer process during laser irradiation on the living biological tissues. The authors implemented the L1 approximation for the Caputo time fractional derivative. At the same time, they also applied central difference scheme for the Riesz fractional derivative to solve their problem. Effects of time and phase lag time, space fractional parameters and blood perfusion rate on temperature distribution within living biological tissues have been examined by numerical simulations and graphical illustrations. Other interesting results about the fractional heat conduction equation can be found in the papers [15,16].

The aim of this paper is to investigate unsteady axial symmetric flows of incompressible and electrically conducting Casson fluids over a vertical cylinder with time-variable temperature, under influence of an external transversely magnetic field. The thermal transport is described by a generalized mathematical model based on the time-fractional differential equation of Cattaneo's law with the Caputo derivative. In this way, our model

is able to highlight the effect of the temperature gradient history on heat transport and fluid motion. The generalized mathematical model of thermal transport can be particularized to obtain the classical Cattaneo's law, respectively the classical Fourier's law.

In this article, we used the Caputo fractional derivative because many theoretical and experimental studies have shown that mathematical models based on this fractional derivative lead to results that are in good agreement with the theoretical results. However, in a later study, the authors intend to study a model based on the generalized Atangana-Baleanu derivative [17]. This fractional derivative generates by particularization the Caputo, Caputo-Fabrizio and Atangana-Baleanu derivatives. The study of such a model will lead to a good comparison between the described model of whole order derivatives and the four fractional derivatives.

The effect of the history of the temperature gradient on the thermal transport and the fluid movement has been highlighted by numerical simulations and graphic illustrations by considering the temperature of the cylindrical surface varying exponentially with time. A comparison of the three models, the generalized Cattaneo, the classic Cattaneo, and the Fourier, gives information on the optimal choice of the thermal transport model.

2. Statement of the Problem

Consider the unsteady flow of an incompressible, electrically conducting Casson fluid over a semi-infinite vertical circular cylinder of radius R_0 . The \tilde{z} -axis of a cylindrical coordinate system $(\tilde{r}, \tilde{\varphi}, \tilde{z})$ is taken along the axis of cylinder in the vertical upward direction. The gravitational acceleration \vec{g} is acting downward, $\vec{g} = -g\vec{e}_{\tilde{z}}$ (Figure 1). A magnetic field $\vec{B} = B_0\vec{e}_{\tilde{r}}$, $B_0 = \text{constant}$ is applied to the fluid.

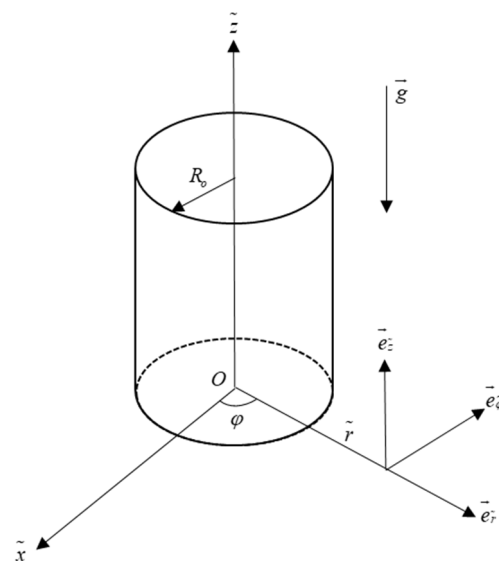


Figure 1. Flow geometry.

The rheological equation of state for the Cauchy stress tensor of Casson fluid is given by

$$\tau_{ij} = \begin{cases} 2\left(\mu_B + \frac{P_y}{\sqrt{2\pi}}\right)e_{ij}, \pi > \pi_c \\ 2\left(\mu_B + \frac{P_y}{\sqrt{2\pi_c}}\right)e_{ij}, \pi < \pi_c \end{cases}, \quad (1)$$

where $\tau = (\tau_{ij})$, $i, j = 1, 2, 3$ is the shear stress tensor, $\pi = e_{ij}e_{ij}$, e_{ij} is the $(ij)^{th}$ component of the deformation rate tensor, π_c is a critical value of the product π , μ_B is a plastic dynamic viscosity of the non-Newtonian fluid,

$$P_y = \frac{\mu_B \sqrt{2\pi}}{\gamma}, \quad (2)$$

where P_y denotes the yield stress of the fluid. If a shear stress less than the yield stress is applied to the fluid it behaves like a solid, whereas if a shear stress greater than yield stress is applied, the fluid starts to move. The non-Newtonian Casson fluids flow if $\pi > \pi_c$. Denoting

$$\mu = \mu_B + \frac{P_y}{\sqrt{2\pi}}, \quad (3)$$

the dynamic viscosity, we obtain the kinematic viscosity

$$v = \frac{\mu}{\rho} = \frac{\mu_B + \frac{P_y}{\sqrt{2\pi}}}{\rho} = \frac{\mu_B + \frac{1}{\gamma}\mu_B}{\rho} = \frac{\mu_B}{\rho} \left(1 + \frac{1}{\gamma}\right), \quad (4)$$

where ρ is the mass density and γ is called the Casson parameter.

In this paper, we consider the velocity field of the form $\vec{v}(\tilde{r}, \tilde{\varphi}, \tilde{z}, \tilde{t}) = \tilde{u}(\tilde{r}, \tilde{t}) \vec{e}_{\tilde{z}}$. The fluid temperature \tilde{T} is considered as function of (\tilde{r}, \tilde{t}) , therefore $\tilde{T} = \tilde{T}(\tilde{r}, \tilde{t})$, and the heat flux vector is given by $\vec{q} = \tilde{q}(\tilde{r}, \tilde{t}) \vec{e}_{\tilde{r}}$. Taking into consideration the above assumption and the Boussinesq's approximation, the flow and heat transfer are governed by the following partial differential equations [1, 2]:

The continuity equation

$$\frac{1}{\tilde{r}} \frac{\partial(\tilde{r}u_{\tilde{r}})}{\partial \tilde{r}} + \frac{1}{\tilde{r}} \frac{\partial u_{\tilde{\varphi}}}{\partial \tilde{\varphi}} + \frac{\partial u_{\tilde{z}}}{\partial \tilde{z}} = 0 \quad (5)$$

The \tilde{z} -component of the linear momentum equation

$$\frac{\partial \tilde{u}(\tilde{r}, \tilde{t})}{\partial \tilde{t}} = \nu \left(1 + \frac{1}{\gamma}\right) \frac{1}{\tilde{r}} \frac{\partial}{\partial \tilde{r}} \left(\tilde{r} \frac{\partial \tilde{u}(\tilde{r}, \tilde{t})}{\partial \tilde{r}} \right) + g\beta \left(\tilde{T}(\tilde{r}, \tilde{t}) - \tilde{T}_{\infty} \right) - \frac{\sigma B_0^2}{\rho} \tilde{u}(\tilde{r}, \tilde{t}) \quad (6)$$

The balance energy equation

$$\rho c_p \frac{\partial \tilde{T}(\tilde{r}, \tilde{t})}{\partial \tilde{t}} = -\text{div} \vec{q} \quad (7)$$

The Cattaneo-Vernotte's constitutive equation

$$\vec{q}(\tilde{r}, \tilde{t}) + \tau_q \frac{\partial \vec{q}(\tilde{r}, \tilde{t})}{\partial \tilde{t}} = -k \text{grad}(\tilde{T}(\tilde{r}, \tilde{t})), \quad (8)$$

where β is the thermal expansion coefficient, σ is the electrical conductivity of the fluid, c_p is the specific heat, τ_q is the thermal relaxation time and k is the thermal conductivity of the fluid. Under the velocity field assumption, we have $u_{\tilde{r}} = 0$, $u_{\tilde{\varphi}} = 0$, $u_{\tilde{z}} = \tilde{u}(\tilde{r}, \tilde{t})$, therefore the continuity Equation (5) is identically satisfied.

The divergence operator in cylindrical coordinate is $\text{div} \vec{q} = \frac{1}{\tilde{r}} \frac{\partial}{\partial \tilde{r}}(\tilde{r}q_{\tilde{r}}) + \frac{1}{\tilde{r}} \frac{\partial q_{\tilde{\varphi}}}{\partial \tilde{\varphi}} + \frac{\partial q_{\tilde{z}}}{\partial \tilde{z}}$. Since $q_{\tilde{r}} = \tilde{q}(\tilde{r}, \tilde{t})$, $q_{\tilde{\varphi}} = 0$, $q_{\tilde{z}} = 0$, we obtain

$$\text{div} \vec{q} = \frac{1}{\tilde{r}} \frac{\partial}{\partial \tilde{r}}(\tilde{r}\tilde{q}(\tilde{r}, \tilde{t})). \quad (9)$$

Also, $grad\tilde{T}(\tilde{r}, \tilde{t}) = \frac{\partial\tilde{T}(\tilde{r}, \tilde{t})}{\partial\tilde{r}} \vec{e}_{\tilde{r}} + \frac{1}{\tilde{r}} \frac{\partial\tilde{T}(\tilde{r}, \tilde{t})}{\partial\tilde{\varphi}} \vec{e}_{\tilde{\varphi}} + \frac{\partial\tilde{T}(\tilde{r}, \tilde{t})}{\partial\tilde{z}} \vec{e}_{\tilde{z}}$. Therefore,

$$grad\tilde{T}(\tilde{r}, \tilde{t}) = \frac{\partial\tilde{T}(\tilde{r}, \tilde{t})}{\partial\tilde{r}} \vec{e}_{\tilde{r}}. \tag{10}$$

Along with the above equation, we consider the initial-boundary conditions

$$\begin{aligned} \tilde{u}(\tilde{r}, 0) &= 0, \quad \tilde{T}(\tilde{r}, 0) = \tilde{T}_{\infty}, \quad \tilde{q}(\tilde{r}, 0) = 0, \quad \tilde{r} \in [R_0, \infty), \\ \tilde{u}(R_0, \tilde{t}) &= 0, \quad \tilde{T}(R_0, \tilde{t}) = \tilde{T}_{\infty} + \tilde{T}_{\infty} f_1(\tilde{t}), \quad \tilde{t} > 0, \\ \tilde{u}(\tilde{r}, \tilde{t}) &\rightarrow 0, \quad \tilde{T}(\tilde{r}, \tilde{t}) \rightarrow \tilde{T}_{\infty} \text{ as } \tilde{r} \rightarrow \infty. \end{aligned} \tag{11}$$

In the above relations function $f_1(\tilde{t})$ is a piecewise function of exponential order to infinity. Using the following dimensionless parameters and functions,

$$\begin{aligned} r = \frac{\tilde{r}}{R_0}, \quad t = \frac{v\tilde{t}}{R_0^2}, \quad u = \frac{R_0\tilde{u}}{v}, \quad T = \frac{\tilde{T} - \tilde{T}_{\infty}}{\tilde{T}_{\infty}}, \quad q = \frac{R_0\tilde{q}}{k\tilde{T}_{\infty}}, \quad Gr = \frac{g\beta\tilde{T}_{\infty}R_0^3}{v^2}, \\ Ha = B_0R_0\sqrt{\frac{\sigma}{\mu}}, \quad \tau = \frac{v\tau_q}{R_0^2}, \quad Pr = \frac{\mu c_p}{k}, \quad f(t) = f_1\left(\frac{R_0^2 t}{v}\right), \end{aligned} \tag{12}$$

We obtain the non-dimensional equations:

$$\frac{\partial u}{\partial t} = \left(1 + \frac{1}{\gamma}\right) \frac{1}{r} \frac{\partial}{\partial r} \left(r \frac{\partial u}{\partial r}\right) + GrT - Ha^2u \tag{13}$$

$$q + \tau \frac{\partial q}{\partial t} = -\frac{\partial T}{\partial r} \tag{14}$$

$$Pr \frac{\partial T}{\partial t} = -\frac{1}{r} \frac{\partial}{\partial r} (rq) \tag{15}$$

The non-dimensional forms of Equation (11) are

$$u(r, 0) = 0, \quad T(r, 0) = 0, \quad q(r, 0) = 0, \quad r \in [1, \infty), \tag{16}$$

$$u(1, t) = 0, \quad T(1, t) = f(t), \quad \lim_{r \rightarrow \infty} u(r, t) = 0, \quad \lim_{r \rightarrow \infty} T(r, t) = 0, \tag{17}$$

The Generalized Fractional Mathematical Model

In this paper, we consider a generalized Cattaneo’s law given by the constitutive equation of the thermal flux,

$$q(r, t) + \tau_0^C D_t^\alpha q(r, t) = -\frac{\partial T(r, t)}{\partial r}, \quad \alpha \in (0, 1] \tag{18}$$

where $D_t^\alpha q(r, t)$ denotes the Caputo time-fractional derivative operator defined as [18,19]

$${}_0^C D_t^\alpha q(r, t) = \begin{cases} \frac{1}{\Gamma(1-\alpha)} \int_0^t (t-\sigma)^{-\alpha} \dot{q}(r, \sigma) d\sigma, & 0 \leq \alpha < 1, \\ \frac{\partial q(r, t)}{\partial t} = \dot{q}(r, t), & \alpha = 1. \end{cases} \tag{19}$$

Let ${}^C h(\alpha, t)$ be the Caputo kernel given by

$${}^C h(\alpha, t) = \frac{t^{-\alpha}}{\Gamma(1-\alpha)}, \quad 0 \leq \alpha < 1. \tag{20}$$

Using (19) and (20), the time-fractional Caputo derivative is written as a convolution, namely,

$${}_0^C D_t^\alpha q(r, t) = {}^C h(r, t) * \frac{\partial q(r, t)}{\partial t}. \tag{21}$$

Using (19), (21) and the properties of the Laplace transform [20], we obtain

$$L\{ {}_0^C D_t^\alpha q(r,t) \} = L\{ {}^C h(r,t) \} \cdot L\left\{ \frac{\partial q(r,t)}{\partial t} \right\} = \frac{1}{s^{1-\alpha}} [sL\{q(x,t)\} - q(r,0)] = s^\alpha \hat{q}(r,s) - s^{\alpha-1} q(r,0), \quad \alpha \in [0,1], \quad (22)$$

where $\hat{q}(r,s) = L\{q(r,t)\} = \int_0^\infty q(r,t)e^{-st} dt$ denotes the Laplace transform of function $q(r,t)$.

3. Solution of the Generalized Mathematical Model

To determine the solution of the proposed problem, the Laplace transform and Bessel functions are used.

3.1. Solution of the Generalized Thermal Process

In this section, we find the solution of the Equations (15) and (18) along with the initial and boundary conditions

$$T(r,0) = 0, \quad q(r,0) = 0 \quad (23)$$

$$T(1,t) = f(t), \quad \lim_{r \rightarrow \infty} T(r,t) = 0, \quad t > 0. \quad (24)$$

Applying the Laplace transform to Equations (15) and (18) and using (22) and (23) we obtain the transformed equations

$$\text{Prs} \hat{T}(r,s) = -\frac{1}{r} \frac{\partial}{\partial r} (r \hat{q}(r,s)) \quad (25)$$

$$(1 + \tau s^\alpha) \hat{q}(r,s) = -\frac{\partial \hat{T}(r,s)}{\partial r}. \quad (26)$$

The Laplace transform $\hat{T}(r,s)$ has to satisfy the boundary conditions

$$\hat{T}(1,s) = \hat{f}(s), \quad \lim_{r \rightarrow \infty} \hat{T}(r,s) = 0. \quad (27)$$

Eliminating $\hat{q}(r,s)$ between Equations (25) and (26) we have that $\hat{T}(r,s)$ satisfies the differential equation

$$\theta(s) \hat{T}(r,s) = \frac{1}{r} \frac{\partial}{\partial r} \left(r \frac{\partial \hat{T}(r,s)}{\partial r} \right), \quad (28)$$

where

$$\theta(s) = \text{Prs}(1 + \tau s^\alpha). \quad (29)$$

Equation (28) is written in the equivalent form

$$r^2 \frac{\partial^2 \hat{T}(r,s)}{\partial r^2} + \frac{\partial \hat{T}(r,s)}{\partial r} - \left(r \sqrt{\theta(s)} \right)^2 \hat{T}(r,s) = 0, \quad (30)$$

that is a modified Bessel equation with the general solution [21,22],

$$\hat{T}(r,s) = A(s) I_0 \left(r \sqrt{\theta(s)} \right)^2 + B(s) K_0 \left(r \sqrt{\theta(s)} \right), \quad (31)$$

where $I_0(z)$, $K_0(z)$ are the modified Bessel functions of the first and second kind of order zero, and $A(s)$, $B(s)$ will be determined from the boundary conditions.

Since $\lim_{r \rightarrow \infty} I_0(r\sqrt{\theta(s)}) = +\infty$ and $\lim_{r \rightarrow \infty} K_0(r\sqrt{\theta(s)}) = 0$, we must consider $A(s) = 0$ in order to have a finite temperature for $r \rightarrow \infty$. Now, using the second boundary condition (27), we obtain the following form of the transformed temperature:

$$\hat{T}(r, s) = \hat{f}(s) \frac{K_0(r\sqrt{\theta(s)})}{K_0(\sqrt{\theta(s)})}. \tag{32}$$

Because the inverse Laplace transform of function (32) cannot be obtained in a simple analytical form, the numerical values of the temperature $T(r, t) = L^{-1}\{\hat{T}(r, s)\}$ are determined by using the Stehfest’s algorithm [23]. According with Stehfest’s algorithm, the temperature is approximated by

$$T(r, t) \simeq \frac{\ln 2}{t} \sum_{j=1}^{2n} D_j \hat{T}\left(r, j \frac{\ln 2}{t}\right), \tag{33}$$

where

$$D_j = (-1)^{j+n} \sum_{i=\lfloor \frac{j+1}{2} \rfloor}^{\min(j,n)} \frac{i^n (2i)!}{(n-i)! i! (i-1)! (j-i)! (2i-j)!}. \tag{34}$$

In the above relations, $[x]$ denotes the integer part of $x \in \mathbb{R}$, and n is an integer positive number.

Let’s note that for $\alpha \in (0, 1)$ and $\tau > 0$, the solutions (32) and (33) give the temperature field corresponding to the generalized fractional Cattaneo thermal process. If $\alpha = 1$ and $\tau > 0$, Equations (32) and (33) give the temperature of the classical Cattaneo thermal process. For $\tau = 0$, Equations (32) and (33) are the solutions of the thermal process described by the classical Fourier’s law.

3.2. Fluid Velocity

The fluid velocity is given by the solution of differential Equation (13) along with the initial and boundary conditions (16) and (17).

Applying the Laplace transform to Equation (13), using the initial condition (16), and the expression (32) of the temperature we obtain the following equation of the transformed velocity $\hat{u}(r, s)$:

$$\frac{\partial^2 \hat{u}(r, s)}{\partial r^2} + \frac{1}{r} \frac{\partial \hat{u}(r, s)}{\partial r} - \frac{s + Ha^2}{\gamma_0} \hat{u}(r, s) + \frac{Gr}{\gamma_0} \hat{f}(s) \frac{K_0(r\sqrt{\theta(s)})}{K_0(\sqrt{\theta(s)})}, \quad \gamma_0 = 1 + \frac{1}{\gamma}. \tag{35}$$

A particular solution of Equation (35) is given by

$$\hat{u}_p(r, s) = -\frac{Gr \hat{f}(s)}{\gamma_0 \theta(s) - s - Ha^2} \cdot \frac{K_0(r\sqrt{\theta(s)})}{K_0(\sqrt{\theta(s)})} \tag{36}$$

The homogenous equation associated with Equation (35) is the modified Bessel equation

$$r^2 \frac{\partial^2 \hat{u}}{\partial r^2} + r \frac{\partial \hat{u}}{\partial r} - \left(r \sqrt{\frac{s + Ha^2}{\gamma_0}} \right)^2 \hat{u} = 0. \tag{37}$$

whose general solution is

$$\hat{u}_h(r, s) = C(s) I_0\left(r\sqrt{\varphi(s)}\right) + D(s) K_0 r \sqrt{\varphi(s)}, \tag{38}$$

where $\varphi(s) = \frac{s+Ha^2}{\gamma_0}$.

To have the finite velocity for $r \rightarrow \infty$, we must take $C(s) = 0$. The general solution of Equation (35) is

$$\hat{u}(r, s) = D(s)K_0\left(r\sqrt{\varphi(s)} + M(s)K_0r\sqrt{\varphi(s)}\right). \quad (39)$$

where $M(s) = -\frac{Gr\hat{f}(s)}{[\gamma_0\theta(s)-s-Ha^2]K_0(\sqrt{\theta(s)})}$.

Using the boundary condition $\hat{u}(1, s) = 0$, we have

$$D(s) = -\frac{M(s)K_0(\sqrt{\theta(s)})}{K_0(\sqrt{\varphi(s)})} = \frac{Gr\tilde{f}(s)}{[\gamma_0\theta(s) - s - Ha^2]K_0(\sqrt{\varphi(s)})}. \quad (40)$$

The transformed velocity field is given by

$$\hat{u}(r, s) = \frac{Gr\hat{f}(s)}{[\gamma_0\theta(s) - s - Ha^2]} \left[\frac{K_0(r\sqrt{\varphi(s)})}{K_0(\sqrt{\varphi(s)})} - \frac{K_0(r\sqrt{\theta(s)})}{K_0(\sqrt{\theta(s)})} \right]. \quad (41)$$

The numerical values of the velocity field in the real domain are obtained using the Stehfest's algorithm, namely,

$$u(r, t) \simeq \frac{\ln 2}{t} \sum_{j=1}^{2n} D_j \hat{u}\left(x, j \frac{\ln 2}{t}\right), \quad (42)$$

where D_j is given by (34).

4. Discussion

The unsteady axial symmetric flow of an incompressible and electrically conducting Casson fluid over a vertical cylinder with time-variable temperature, in the presence of a transversely applied magnetic field is studied. The temperature of the cylinder surface is described by a function of time that is a piecewise continuous function for $t \in [0, \infty)$ and of exponential order to infinity.

In this study, we have considered a fractional generalized mathematical model based on the time-fractional differential equation of Cattaneo's law with the Caputo derivative. In this way, our model is able to highlight the effect of the temperature gradient history on the heat transport and fluid motion.

The generalized mathematical model of thermal transport can be particularized to obtain the classical Cattaneo' law, when the memory parameter is $\alpha = 1$, respectively the classical Fourier's law when the thermal relaxation time τ is equal to zero. In this way, the comparison of the three models leads to choose the optimal model of the heat transport.

In order to analyze the influence of several system parameters on the heat transfer and fluid flow some numerical simulations are made considering the nondimensional cylinder temperature given by the function $f(t) = 15(1 - e^{-t/10})$ whose Laplace transform is $\hat{f}(s) = \frac{15}{s(10s+1)}$. The numerical results are presented in graphical illustrations in Figures 2–9.

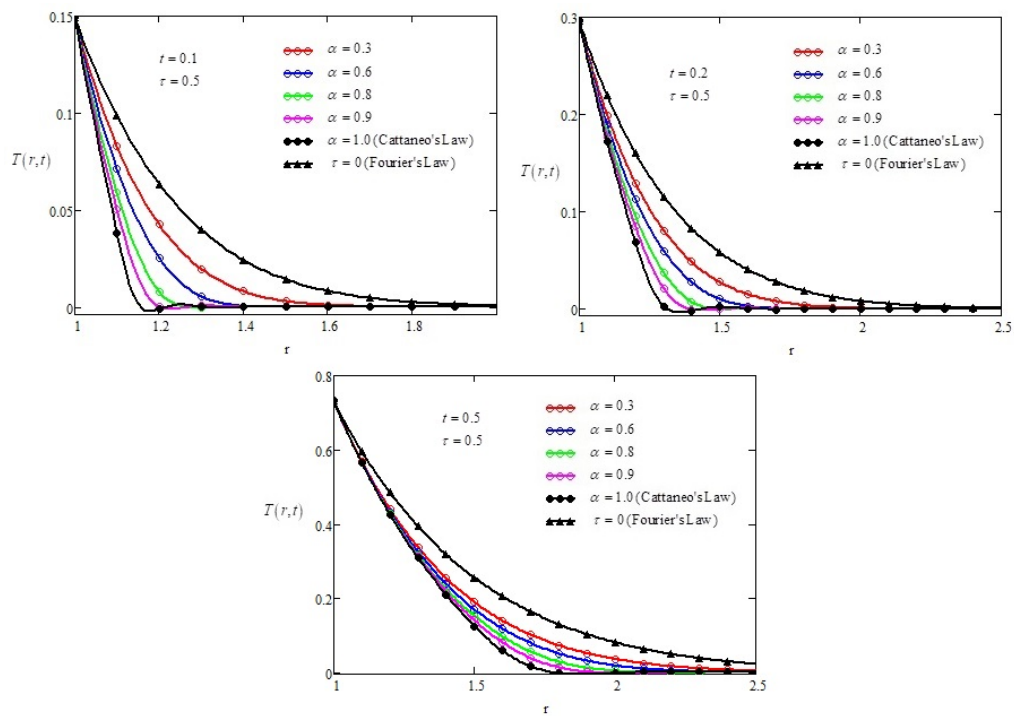


Figure 2. The profiles of the nondimensional temperature $T(r,t)$ for different values of the fractional parameter.

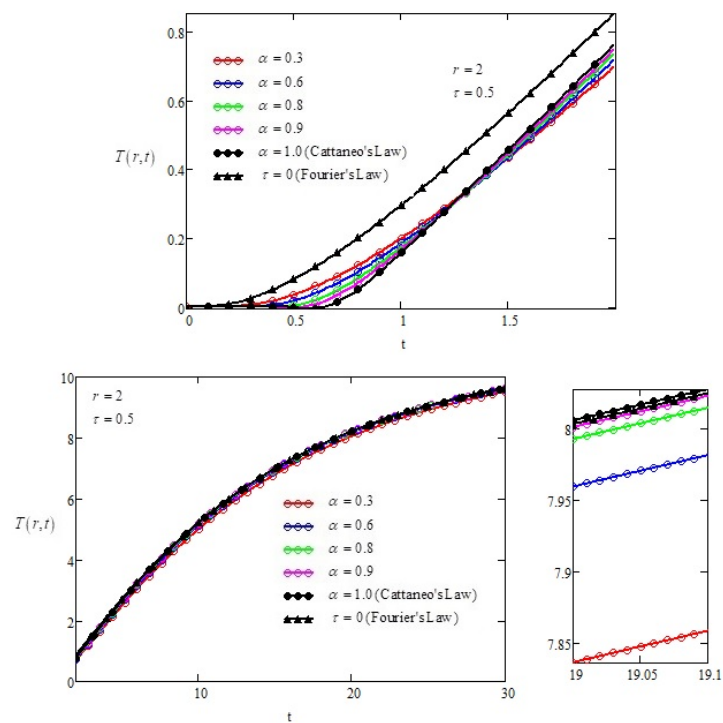


Figure 3. Time-variation of the nondimensional temperature $T(r,t)$ for different values of the fractional parameter.

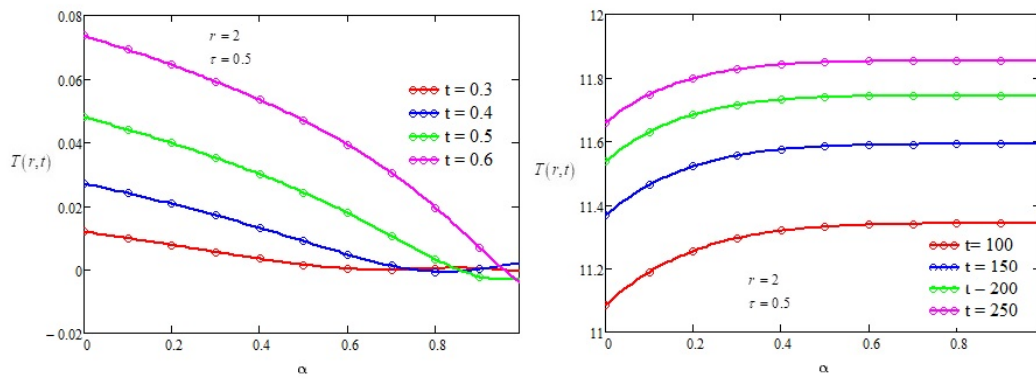


Figure 4. The influence of the fractional parameter α for different values of the fractional parameter.

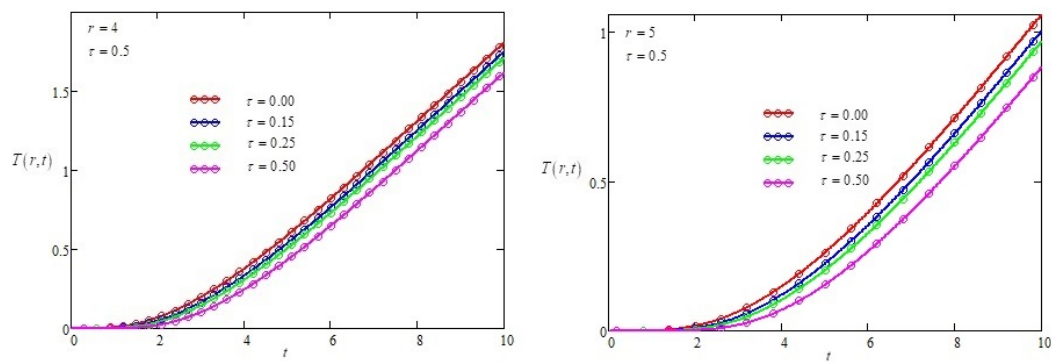


Figure 5. The influence of the thermal relaxation τ on the temperature field.

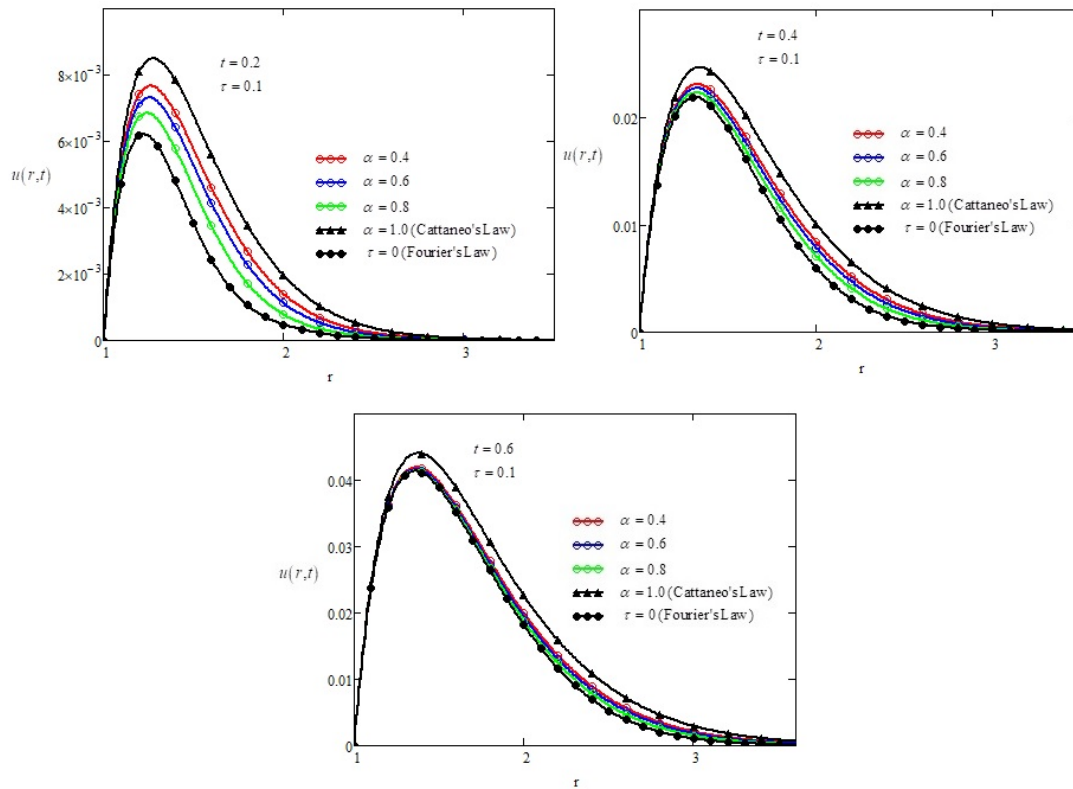


Figure 6. Velocity profiles $u(r,t)$ versus r for different values of the fractional parameter α .

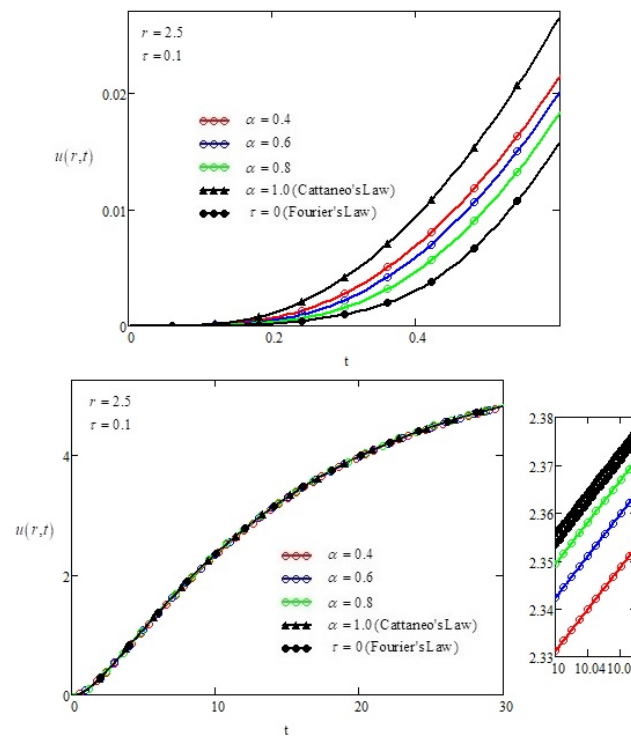


Figure 7. Time variation of the fluid velocity $u(r, t)$.

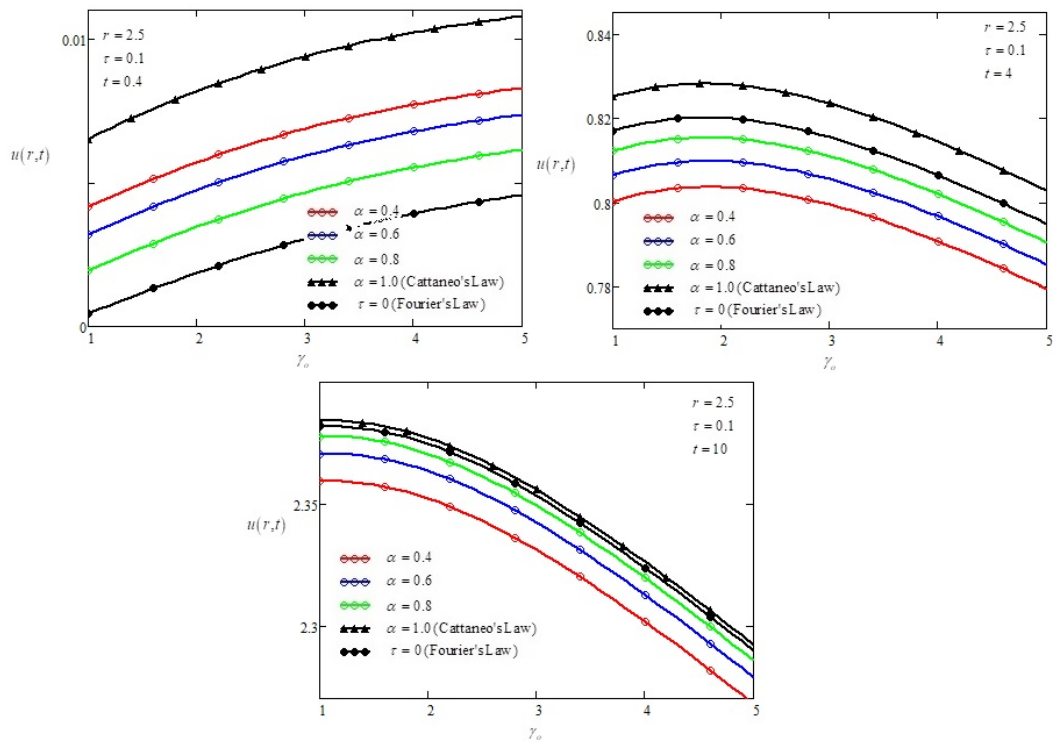


Figure 8. The variation of the fluid velocity with the Casson parameter γ_0 .

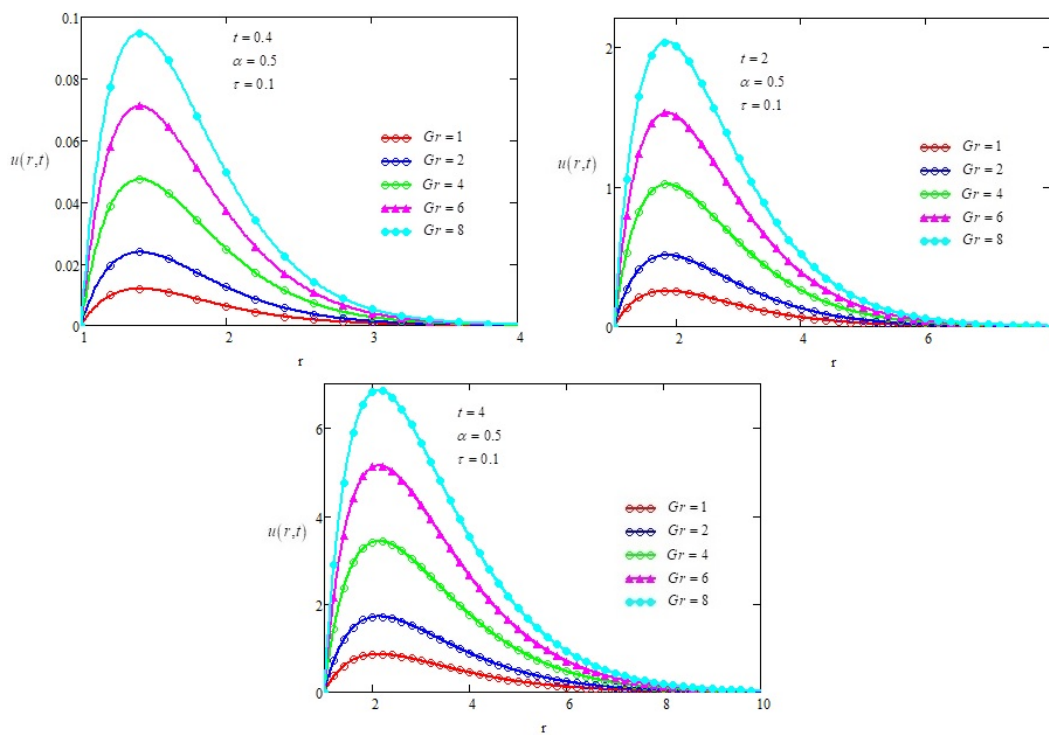


Figure 9. The influence of Grashof number Gr on the fluid velocity.

The variation of the dimensionless temperature $T(r, t)$, for small values of time and for different values of the fractional parameter α are shown in Figure 2. The temperature profiles were drawn for three cases corresponding to the fractional mathematical model but also for the classic cases of thermal transport Cattaneo, respectively Fourier.

As expected, the Fourier heat transfer model generates higher temperatures than the fractional and classic Cattaneo models. This is due to the fact that in the case of the latter models the history of the temperature gradient influences the evolution in time of the thermal flux, so the whole process of thermal transport. It should also be noted that the weight function that affects the temperature gradient in the case of the classic Cattaneo model is $k_1(t) = \exp(-t/\tau)$, while in the fractional Cattaneo model it is $k_2(t) = t^{\alpha-1}E_{\alpha,\alpha}(-t^\alpha/\tau)$, where, $E_{\alpha,\beta}(\cdot)$ is two-parameters Mittag-Leffler function [24]. Obviously, $\lim_{\alpha \rightarrow 1} k_2(t) = k_1(t)$. This is visible in Figure 2 where, for $\alpha = 0.9$ the temperature profile is close to that corresponding to $\alpha = 1$.

The time variation of the nondimensional temperature $T(r, t)$ is shown in Figure 3. As we discussed results obtained in Figure 2, it is more clearly in Figure 3 that the memory effects have different influences for small values of time, respectively large values of the time t . It is observed in Figure 3 that at small values of the time t , the fractional Cattaneo’s law leads to higher temperatures than that corresponding to the classical Cattaneo’s law, but, for large values of time, the fractional models generate the smallest temperatures. Moreover, for high values of time t , the temperature field tends to have a constant value. This value is the same for all the analyzed models. On the one hand, this property results from numerical simulation, but it can also be justified theoretically using the following property:

$$\lim_{t \rightarrow \infty} f(t) = \lim_{s \rightarrow 0} s \hat{f}(s) \tag{43}$$

Using Equation (32) and the property (43), we obtain

$$\lim_{t \rightarrow \infty} T(r, t) = \lim_{s \rightarrow 0} s \hat{f}(s) \frac{K_0(r\sqrt{\theta(s)})}{K_0(\sqrt{\theta(s)})} = \lim_{t \rightarrow \infty} f(t) \lim_{s \rightarrow 0} \frac{K_0(r\sqrt{\theta(s)})}{K_0(\sqrt{\theta(s)})} \tag{44}$$

Using the asymptotic approximations of Bessel functions [25]

$$K_\nu(z) = \begin{cases} -\gamma - \ln \frac{z}{2}, \nu = 0, \\ \frac{\Gamma(\nu)}{2} \left(\frac{z}{2}\right)^\nu, \nu > 0, \end{cases} \tag{45}$$

if $0 < z < \sqrt{\nu + 1}$, we get $\lim_{s \rightarrow 0} \frac{K_0(r\sqrt{\theta(s)})}{K_0(\sqrt{\theta(s)})} = 1$, therefore, $\lim_{t \rightarrow \infty} T(r, t) = \lim_{t \rightarrow \infty} f(t)$. In the considered case $\lim_{t \rightarrow \infty} T(r, t) = \lim_{t \rightarrow \infty} f(t) = 15$.

The variation of dimensionless temperature $T(r, t)$ with the fractional parameter α is shown in Figure 4. It is seen in this figure that the temperature is increasing with the fractional parameter. However, for high values of time, the influence of the fractional parameter on the temperature is insignificant. This is due to the time evolution of the fractional kernel $k_2(t)$ that decreases to zero when $t \rightarrow \infty$. The influence of the thermal relaxation time on the thermal field is shown in Figure 5. It is seen that the temperature decreases with the relaxation time τ .

Fluid motion is analyzed by the graphs in Figures 6–9. Figure 6 shows the velocity profiles versus the radial variable r , for different values of the fractional parameter α . It is observed that there is a perfect correlation between the evolution of fluid temperature and velocity concerning the memory parameter α , namely, the velocity values decrease with the memory parameter α . On the other hand, the velocity has a maximum value near the cylindrical surface and tends to zero away from it.

Figure 7 shows the time variation of the fluid velocity in several spatial positions for different values of the time-variation. As in the case of temperature, for small values of time, the influence of thermal memory is significant, but it decreases for large values of time. Note that using Equations (41) and (43), we obtain the following expression for the velocity of the fluid for high values of time t :

$$\lim_{t \rightarrow \infty} u(r, t) = \lim_{s \rightarrow 0} s\hat{u}(r, s) = \frac{Gr}{Ha^2} \left(1 - \frac{K_0(rHa/\sqrt{\gamma_0})}{K_0(Ha/\sqrt{\gamma_0})} \right) \lim_{t \rightarrow \infty} f(t) \tag{46}$$

The influence of the Casson parameter γ_0 on the fluid motion is shown in Figure 8. It can be seen that at low values of time, the fluid velocity is increasing with the Casson parameter γ_0 , but has an opposite character for high values of the Casson parameter. This fact is due to for increasing of Casson parameter the fluid viscosity increases, therefore the fluid motion is slowed down.

Figure 9 is drawn to highlight the influence of the Grashof number on fluid motion. Note that the fluid velocity increases with the Grashof number. This is obvious because increasing the value of the Grashof number leads to an increase in buoyancy.

Author Contributions: Conceptualization, Z.I. and D.V.; methodology, H.I.O.; software, H.I.O.; validation, H.I.O., D.V. and Z.I.; formal analysis, D.V.; investigation, Z.I.; resources, D.V. and Z.I.; data curation, Z.I.; writing—original draft preparation, H.I.O. and D.V.; writing—review and editing, D.V. and Z.I.; visualization, Z.I.; supervision, Z.I.; project administration, D.V. and Z.I.; funding acquisition, D.V. and Z.I. All authors have read and agreed to the published version of the manuscript.

Funding: This research was funded by UNIVERSITI MALAYSIA PAHANG (CRG UTP) through the vote RDU213207.

Institutional Review Board Statement: Not applicable.

Informed Consent Statement: Not applicable.

Data Availability Statement: Not applicable.

Acknowledgments: The authors would like to acknowledge Universiti Malaysia Pahang (UMP) for the financial support via vote number RDU213207 and Post Graduate Research Scheme (PGRS210329) for this research.

Conflicts of Interest: The authors declare no potential conflict of interest.

References

1. Casson, N. A flow equation for pigment-oil suspensions of the printing ink type. In *Rheology of Disperse Systems*; Pergamon Press: Oxford, UK, 1959; pp. 84–104.
2. Alwawi, F.A.; Hamarshah, A.S.; Alkawasbeh, H.T.; Idris, R. Mixed convection flow of magnetized Casson nanofluid over a cylindrical surface. *Coatings* **2022**, *12*, 296. [[CrossRef](#)]
3. Kumar, G.; Rizvi, S.M.K. Casson fluid flow past on vertical cylinder in the presence of chemical reaction and magnetic field. *Appl. Appl. Math. Int. J.* **2021**, *16*, 524–537.
4. Reddy, G.J.; Kethireddy, B.; Kumar, M.; Beg, O.A. Transient analysis of Casson fluid thermo-convection from a vertical cylinder embedded in a porous medium: Entropy generation and thermal energy transfer visualization. *J. Cent. South Univ.* **2019**, *26*, 1342–1361. [[CrossRef](#)]
5. Khan, S.; Selim, M.M.; Gepreel, K.A.; Ullah, A.; Ayaz, M.; Mashwani, W.K.; Khan, E. An analytical investigation of the mixed convective Casson fluid flow past a yawed cylinder with heat transfer analysis. *Open Phys.* **2021**, *19*, 0040. [[CrossRef](#)]
6. Sarkar, T.; E-Rabbi, S.R.; Arifuzzaman, S.M.; Ahmed, R.; Khan, M.S.; Ahmmmed, S.F. MHD radiative flow of Casson and Williamson nanofluids over an inclined cylindrical surface with chemical reaction effects. *Int. J. Heat Technol.* **2019**, *37*, 1117–1126. [[CrossRef](#)]
7. Naqvi, S.M.R.S.; Muhammad, T.; Asma, M. Hydromagnetic flow of Casson nanofluid over a porous stretching cylinder with Newtonian heat and mass conditions. *Phys. A* **2020**, *550*, 123988. [[CrossRef](#)]
8. Ullah, I.; Alkanhal, T.A.; Shafie, S.; Nisar, K.S.; Khan, I.; Makinde, O.D. MHD Slip Flow of Casson fluid along a nonlinear permeable stretching cylinder saturated in a porous medium with chemical reaction, viscous dissipation, and heat generation/absorption. *Symmetry* **2019**, *11*, 531. [[CrossRef](#)]
9. Szymanek, E. Use the fractional calculus in modeling of heat transfer process through external building partitions. *Acta Innov.* **2018**, *27*, 61–70. [[CrossRef](#)]
10. Povstenko, Y.Z. Fractional heat conduction equation and associated thermal stress. *J. Therm. Stress.* **2005**, *28*, 83–102. [[CrossRef](#)]
11. Dhar, A.; Kundu, A.; Kundu, A. Anomalous heat transport in one dimensional systems: A description using non-local fractional-type diffusion equation. *Front. Phys.* **2019**, *7*, 159. [[CrossRef](#)]
12. Kukla, S.; Siedlecka, U. A fractional single-phase-lag model of heat conduction for describing propagation of the maximum temperature in a finite medium. *Entropy* **2018**, *20*, 876. [[CrossRef](#)] [[PubMed](#)]
13. Liu, Y.; Chi, X.; Xu, H.; Jiang, X. Fast method and convergence analysis for the magnetohydrodynamic flow and heat transfer of Maxwell fluids. *Appl. Math. Comput.* **2022**, *430*, 127255. [[CrossRef](#)]
14. Wang, X.; Qi, H.; Yang, X.; Xu, H. Analysis of the time-space fractional bioheat transfer equation for biological tissues during laser irradiation. *Int. J. Heat Mass Transf.* **2021**, 121555. [[CrossRef](#)]
15. Zecova, M.; Terpak, J. Heat conduction modeling by using fractional-order derivatives. *Appl. Math. Comput.* **2015**, *257*, 365–373.
16. Saqib, M.; Khan, I.; Shafie, S. Application of fractional differential equations to heat transfer in hybrid nanofluid: Modeling and solution via integral transforms. *Adv. Differ. Equ.* **2019**, *52*, 1–18. [[CrossRef](#)]
17. Vieru, D.; Fetecau, C.; Ahmed, N.; Shah, N.A. A kinetic generalized model of the advection-dispersion process in a sorbing medium. *Math. Model. Nat. Phenom.* **2021**, *16*, 39. [[CrossRef](#)]
18. Caputo, M. Linear model of dissipation whose Q is almost frequency independent-II. *Geophys. J. Int.* **1967**, *13*, 529–539. [[CrossRef](#)]
19. Tarasov, V.E. *Fractional Dynamics: Applications of Fractional Calculus to Dynamics of Particles, Fields and Media*; Springer Science & Business Media: Berlin/Heidelberg, Germany, 2010.
20. Eiderman, V. *An Introduction to Complex Analysis and the Laplace Transform*; Chapman & Hall/CRC Press: Boca Raton, FL, USA, 2021.
21. Watson, G.N. *A Treatise on the Theory of Bessel Functions*; Cambridge University Press: Cambridge, UK, 1995.
22. Korenev, B.G. *Bessel Functions and Their Applications*; CRC Press: Boca Raton, FL, USA, 2002.
23. Kuznetsov, A. On the convergence of the Gaver-Stehfest algorithm. *SIAM J. Numer. Anal.* **2013**, *51*, 2984–2998. [[CrossRef](#)]
24. Gorenflo, R.; Kilbas, A.A.; Mainardi, F.; Rogosin, S.V. *Mittag-Leffler Functions, Related Topics and Applications*; Springer: New York, NY, USA, 2014.
25. Sidi, A.; Hoggan, P.E. Asymptotics of modified Bessel functions of high orders. *Int. J. Pure Appl. Math.* **2011**, *71*, 481–498.